ChemComm

Accepted Manuscript

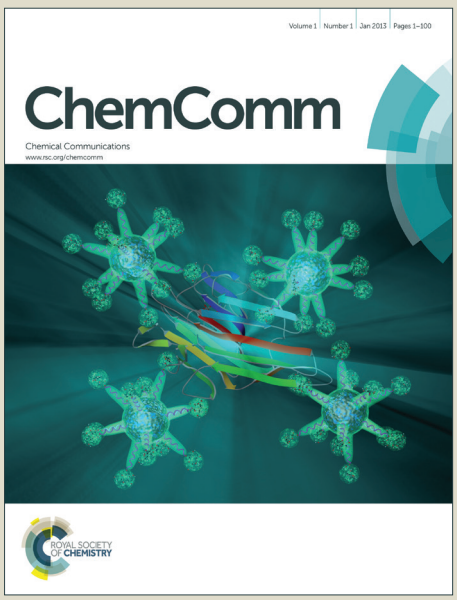

ROYAL SOCIETY OF CHEMISTRY

www.rsc.org/chemcomm

Cite this: DOI: 10.1039/c0xx00000x

www.rsc.org/xxxxxx

ARTICLE TYPE

A sensitive colorimetric strategy for sensitively monitoring cerebral β-amyloid peptides in AD based on dual-functionalized gold nanoplasmic particles †

Yan-yan Yu,[ab1] Lin Zhang,[b1] Xiao-yu Sun,[b] Cheng-lin Li,[b] Yu Qiu,[c] Hao-peng Sun,[d] Dao-quan Tang,[ab] Yao-wu Liu[b] and Xiao-xing Yin*[b]

Received (in XXX, XXX) Xth XXXXXXXXX 20XX, Accepted Xth XXXXXXXXX 20XX

DOI: 10.1039/b000000x

A sensitive and selective strategy for the colorimetric visualization of total monomeric Aβ down to 40 pg mL^{-1} based on dual-functionalized gold nanoplasmic particles (GNPs) is developed and applied to evaluate Aβ levels in AD cerebral system.

Alzheimer's disease (AD) is a multifaceted neurodegenerative disorder characterized by protein misfolding and aggregation, oxidative stress, mitochondrial abnormalities, and neuroinflammatory processes.[1] Intracellular β-amyloid peptide (Aβ) and its aggregates are thought to be responsible for the disease pathology.[2] In its native form, Aβ is disordered but it aggregates into a β-sheet structure of ordered fibrils under various conditions.[3] Currently, selectively and quantitatively measuring Aβ in biological solutions is crucial and helpful in AD clinical studies.[4]

Heme (ferriprotoporphyrin IX) metabolism appears altered in the brains of AD patients, which behaves as that heme oxygenase (HO) and the level of bilirubin both increase in AD patients.[5] Recent studies have invoked that heme is associated with AD by binding to Aβ to form an Aβ-heme complex with a high affinity, which can stabilize the structure of Aβ and inhibite Aβ aggregation.[6] Meanwhile, peptides are very effective and often specific ligands for a variety of transition metal ions and all the metal binding sites are present in the N-terminal hydrophilic region of the Aβ peptide (i.e. within the 1st 16 amino acids).[7] In the case of Cu^{2+}, a large body of evidence has been accumulated supporting an important role of this metal ion in the metabolism of Aβ linked to AD. Initial studies have indicated that the Cu^{2+} bound Aβ peptide has a 3N[8] and 1O coordination environment, in which the 3N coornination was either from three histidine residues[9] or two histidine residues and the N-terminus of the peptide.[10] However, Pramanik's group have illustrated in their recent study that Cu^{2+} cannot bind to three histidine residues simultaneously in Cu-Aβ complex as previously proposed, since one of the histidine is involved in binding heme.[11]

Colorimetric methods, which take advantage of the color change that arises from the interparticle plasmon coupling during the aggregation of gold nanoplasmonic particles (GNPs) or the redispersion of GNP aggregates, have become an efficient approach to monitor the dynamics of biological events due to their biocompatibility, photostability, and superior optical properties.[12,13] In the present work, we propose a rapid, sensitive and colorimetric strategy for total monomeric Aβ determination in normal, AD and ginkgo biloba extract (GBE) - treated rat brains on the basis of double interactions between dual-functionalized GNPs and Aβ. To achieve this goal, a dual-functionalized GNPs as the detection nanoprobe is designed by covalently linking both Cu^{2+} and hemin onto the same polyethyleneimine (PEI) - modified GNP surface. Once Aβ species are added into this probe, double molecular recognitions take place between the dual-functionalized GNP and Aβ by forming a Cu-Aβ-hemin complex, resulting in GNPs aggregations and an obvious color change and thereby realizing the direct colorimetric visualization of Aβ. Interestingly, the proposed methodology displays different abilities to sensitize Aβ species among the five Aβ isoforms including $Aβ_{-11}$, $Aβ_{-16}$, $Aβ_{-38}$, $Aβ_{-40}$ and $Aβ_{-42}$ under identical conditions. Notably, this spontaneous interaction between Aβ peptides and Cu and hemin to construct a GNPs-based colorimetric assay is for the first time developed for the sensitive and selective determination of Aβ monomers in a rat cerebral system.

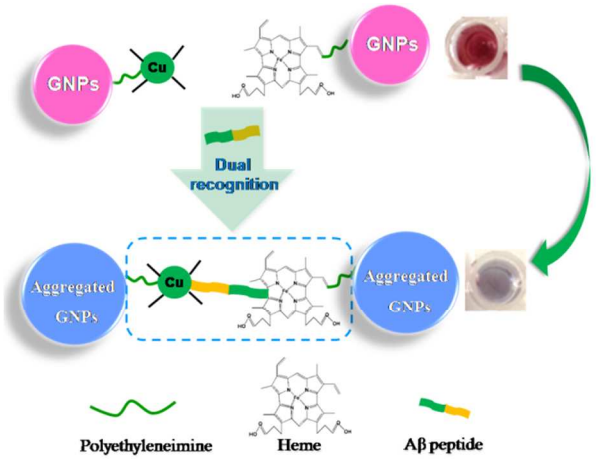

Scheme 1. Colorimetric sensing for Aβ based on the PEI/GNPs-Cu-hemin probe.

Briefly, our technique is simple, fast and only involves incubating the synthesized PEI/GNPs-Cu-hemin probe with Aβ

solution and then observing the color change by our naked eyes (Scheme 1). The characterizations of the probe and the optimizations of experimental conditions are shown in Fig. S3-S4 in ESI†.

As depicted in Fig. S5, the obtained probe presents an absorption peak at 525 nm and wine red in color in the absence of Aβ (black curve and vial 1). No significant change is induced when this probe is incubated for a longer time (2 h) without Aβ addition (red curve), indicating the high stability of the probe under experimental conditions. On the contrary, after an addition of 0.005 mg mL^{-1} $Aβ_{-42}$ into the probe and incubated for 1 h, an obvious decrease in the absorbance at 525 nm is observed and a new absorption peak near 570 nm appears (cyan curve), accompanied with a dramatic color change from wine red to violet blue (vial 2), indicating the aggregations of the probe. Meanwhile, two control experiments, e.g., adding Tris-HCl (pH 7.4) and NaOH solution, solvents for solublizing Aβ, into the probe are performed in the same way as $Aβ_{-42}$. Clearly to be seen, there is not any change in the spectrum in comparison with the original probe (green and blue curves), which further confirms that such a change in the spectrum, along with the apparent color change, can be ascribed to the Aβ induced aggregations of PEI/GNPs-Cu-hemin probe through double molecular recognitions. Moreover, the four UV-vis spectra (Fig. S6 in ESI†) recorded from the four composites of PEI/GNPs, PEI/GNPs-Cu, PEI/GNPs-hemin and the designed probe toward the same concentration of $Aβ_{-42}$ showed that aggregation only happens when the two Aβ recognition elements (Cu^{2+} and hemin) are both modified onto GNPs, indicating the feasibility of this strategy.

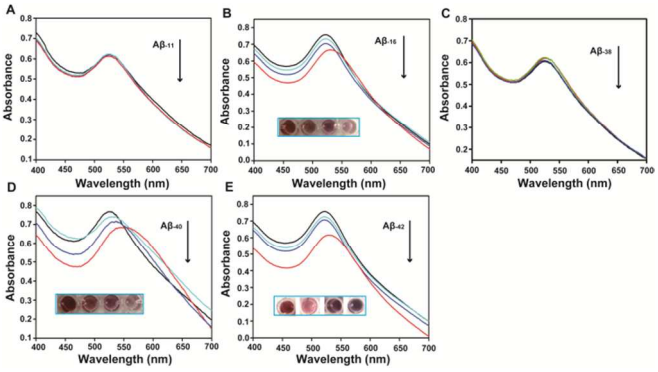

Fig. 1 Typical UV-vis absorption spectra of the designed PEI/GNPs-Cu-hemin probe before (black) and after incubation with different concentrations of (A) $Aβ_{-11}$, (B) $Aβ_{-16}$, (C) $Aβ_{-38}$, (D) $Aβ_{-40}$ and (E) $Aβ_{-42}$. Inset in (B), (D) and (E): direct observations of the color changes following additions of 10^{-6}, 10^{-5} and 10^{-3} mg mL^{-1} $Aβ_{-16}$, $Aβ_{-40}$ and $Aβ_{-42}$ into the probe.

Under the optimized conditions, it is found that the Aβ induced probe aggregation is rather different among five Aβ isoforms, e.g., $Aβ_{-11}$, $Aβ_{-16}$, $Aβ_{-38}$, $Aβ_{-40}$ and $Aβ_{-42}$, which coexist in rat cerebral system. As can be seen from Fig. 1, the initial addition of 10^{-6} mg mL^{-1} $Aβ_{-11}$ into the probe doesn't induce an observable change in the absorption spectrum. Even though the concentration of this peptide increases to 10^{-5} or 10^{-3} mg mL^{-1}, the UV-vis spectrum keeps identical (A). The same thing happens for $Aβ_{-38}$ (C), which declares that under present conditions, the designed probe is unable to recognize the two peptides. Whereas in the incubated solution that contains $Aβ_{-16}$ or $Aβ_{-40}$ or $Aβ_{-42}$, a great similarity in their spectra variations is detected, that is, gradual decrease in the absorbance at 525 nm and a red-shift of the maximum absorption wavelength upon additions of increasing concentrations of $Aβ_{-16}$ or $Aβ_{-40}$ or $Aβ_{-42}$, indicative of a similar discrimination ability among them with the probe (B, D and E). In particular, as compared with the four Aβ isoforms, additions of $Aβ_{-42}$ into the probe induces a much more intense decrease in the spectral absorption at a higher concentration (10^{-3} mg mL^{-1}), although the change is similar to those of $Aβ_{-16}$ and $Aβ_{-40}$ in lower concentrations. Moreover, besides the obvious decrease in the intensity at 525 nm, a detectable red-shift of the absorption peak appeares as GNPs clusters form, accompanied with the visually gradual color change from wine red to pale pink or violet blue (inset in E). These observations reveal the isoform-specific aggregations of the PEI/GNPs-Cu-hemin probe.

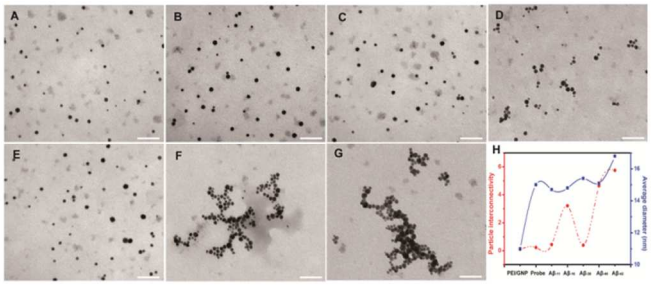

Fig. 2 TEM images of (A) PEI/GNPs, (B) the designed PEI/GNPs-Cu-hemin probe, (C) - (G) the probe incubated with $Aβ_{-11}$, $Aβ_{-16}$, $Aβ_{-38}$, $Aβ_{-40}$ and $Aβ_{-42}$, respectively. (H): corresponding interconnectivity and average diameters of particles in the above seven situations. The scale bars represent 50 nm.

To further confirm the Aβ isoform-specific aggregations of the PEI/GNPs-Cu-hemin probe, transmission electron microscope (TEM) images of the as-prepared probe in the absence and presence of five Aβ isoforms are taken and compared (Fig. 2). As displayed, the pristine PEI modified GNPs are well-dispersed with an average diameter of around 11 nm (A). The functionalizations of PEI/GNPs with Cu and hemin don't alter the original morphology greatly as only a tiny portion of PEI/GNPs is drawn closer to one another and the number of these "aggregated" particles is rather low, but the average particle size increases to 15 nm due to the massive assembly of hemin (B). When $Aβ_{-11}$ or $Aβ_{-38}$ is added into the probe, no further variations in the monodispersity of the probe is observed, as majority of the particles remain isolated from each other (C and E), which is highly consistent with above-mentioned unchanged UV-vis spectra upon additions of $Aβ_{-11}$ and $Aβ_{-38}$. As for $Aβ_{-16}$, a larger number of scattered PEI/GNPs start to coalesce and the degree of particle aggregations extensively ascends (D). Noticeably, remarkable aggregations of PEI/GNPs occur after $Aβ_{-40}$ or $Aβ_{-42}$ is incubated with the probe (F and G). More densely interconnected particles and increased degree of aggregations are both observed in these two situations and in particular, compared with other four isoforms, $Aβ_{-42}$-induced particle aggregations are most profound, not only reflected in the increased number of associated particles, but also the bigger sizes (approximately 17 nm). The corresponding interconnectivity[14] and average

diameters of particles in the seven situations are summarized in Fig. 2H. As reflected, the particle average diameters of the probe both in the absence and presence of five Aβ isoforms keep almost constant in a quite narrow range between 14.7 and 15.4 nm, except for $Aβ_{-42}$, under which situation, the diameter dramatically increases to nearly 17 nm. Whereas for the interconnectivity values, the biggest also corresponds to $Aβ_{-42}$, followed by $Aβ_{-40}$ and $Aβ_{-16}$, indicating $Aβ_{-42}$-induced particle aggregations are most severe among the five isoforms, which is in aggrement with UV-vis results (Fig. 1).

The combined UV-vis and TEM results elaborated above both demonstrate that the degree of aggregation of the PEI/GNPs-Cu-hemin probe is of great difference when different Aβ isoforms are added into the probe. Such a phenomenon may be fairly correlated with the amino acid sequences of Aβ, the simultaneous binding of Aβ with Cu^{2+} and hemin (binding force and binding rate) and the dynamics of GNPs aggregation in a limited space and time. It has been mentioned that the minimal metal-binding site on the Aβ peptide has been identified to consist of the first 16 N-terminal amino acids,[8, 15] possibly due to which, the shorter Aβ peptide with only 11 N-termial amino acids fails in a stable coordination with Cu^{2+} and therefore the double molecular recognitions disappear between the probe and $Aβ_{-11}$. Apart from $Aβ_{-38}$, the other three Aβ isoforms ($Aβ_{-16}$, $Aβ_{-40}$ and $Aβ_{-42}$) don't display differential responses under the identical conditions, indicating that although these Aβs have different amino acid sequences, the binding of them with Cu^{2+} and hemin and the dynamics of GNPs aggregation in the process of binding are rather similar to each other. However, at higher concentrations, $Aβ_{-42}$ induces a more intense aggregation than others, possibly due to the fact that the coordination with metal ions is considered much easier to happen for $Aβ_{-42}$ due to: 1) when more secondary structures (e.g., α-helix and β-sheet) are contained in the peptide, the coordination with metal ions would become much easier;[16] 2) the close relationship with the hydrophobic 20-35 amino acid residues in the C-terminals.[17] The reason for the failure of $Aβ_{-38}$ in causing the probe aggregation is likely that its spatial configuration differs from those of $Aβ_{-16}$, $Aβ_{-40}$ and $Aβ_{-42}$ when binding with Cu^{2+} and hemin, which directly leads to the repelling of GNPs and thus the failure in aggregations. A detailed mechanism still needs to be further explored in our future work.

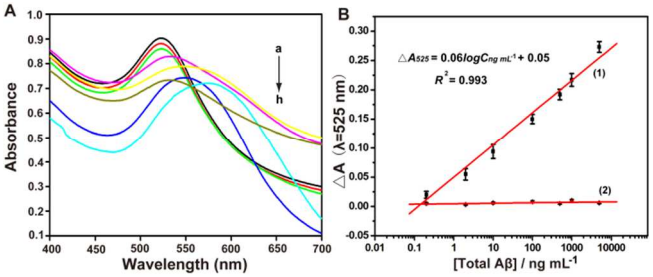

Fig. 3 (A) UV-vis spectra of the designed PEI/GNPs-Cu-hemin probe with the additions of total Aβ monomers at the concentrations of (a-h) 0, 0.2, 2, 10, 100, 500, 1000 and 5000 ng mL^{-1}. (B) Corresponding linear plot of ⊿A at 525 nm *versus* the logarithm of (1) total Aβ monomers and (2) oligomers concentrations. These solutions are prepared by mixing $Aβ_{-16}$, $Aβ_{-40}$ and $Aβ_{-42}$ in a ratio of 3:6:1.[18] $⊿A = A_1 - A_2$, in which A_1 and A_2 represent the absorbances at 525 nm of the probe before and after incubation with Aβ.

The inhibition of the probe aggregation is investigated to further prove the veracity of GNPs based colorimetric asssay (Fig. S7 in ESI†). The probe demonstrates excellent selectivity against endogenic proteins, metal ions and amino acids (Fig. S8 in ESI†). Furthermore, the colorimetric strategy shows a high sensitivity toward total Aβ monomers ($Aβ_{-16}$, $Aβ_{-40}$ and $Aβ_{-42}$) with a wide linear range from 0.2 to 5000 ng mL^{-1} (curve 1, Fig. 3). The detection limit (LOD) of the method, estimated from 3σ of the baseline signals, is approximately 40 pg mL^{-1} for total Aβ monomers, which is similar or superior to those reported for other assays.[4,19] The excellent sensitivity can be ascribed to the significant amplification of GNPs and the highly dual molecule recognition ability of hemin and Cu to Aβ. In addition, the linear plot of total Aβ oligomers shown in Fig. 3 (curve 2) further illustrates that the developed colorimetric method is only suitable for the monitoring of monomeric forms of Aβ, rather than oligomeric or other forms, which indicates that the established colorimetric approach holds great potential for Aβ monomers determination in a complex biological matrix.

Table 1. Evaluation of the variations in total Aβ monomer levels in normal, AD, CMC-Na and GBE-treated rat brains (n = 12, mean ± S.D.).

Aβ content (ng mL^{-1})	CSF	Hippocampus	Prefrontal cortex	Striatum
Normal [a]	29.2 ± 7.6	23.1 ± 5.7	21.9 ± 6.1	17.8 ± 4.7
AD *	22.2 ± 6.0	15.0 ± 4.3	10.6 ± 3.2	7.3 ± 2.5
CMC-Na [b] *	22.7 ± 5.4	14.8 ± 3.5	11.1 ± 2.8	6.8 ± 2.4
GBE **	28.8 ± 7.9	22.8 ± 7.1	22.5± 6.4	16.8 ± 4.3

[a] Untreated healthy rats.

[b] AD rats administrated (i.g.) with CMC-Na daily for two weeks as a control for GBE-treated group.

* $P < 0.0001$ compared with normal group; ** $P < 0.0001$ compared with AD or CMC-Na group.

The proposed methodology is then applied for the evaluations of total monomeric Aβ levels in rat brains. Table 1 lists monomeric Aβ level variations in CSF and brain tissues (hippocampus, prefrontal cortex and striatum) among normal, AD, CMC-Na (control) and (GBE)-treated rats (see experimental section in ESI†). Compared with normal rats, clear declines in the concentration of Aβ monomers in these brain regions of AD and CMC-Na rats are observed due to the aggregations of these peptides as AD progresses ($P < 0.0001$), which is consistent with our previous observations.[20] Following administration of GBE (150 mg kg^{-1}) for two weeks, Aβ concentrations in these brain areas rise again ($P < 0.0001$), benefited from the protective effect of GBE on the damaged neurons in AD brains. The determined results by the present method are compared with those obtained by the conventional ELISA (Table S4 in ESI†), which indicates that the concentrations of Aβ monomers in rat brains determined by the current colorimetric method are in good aggrement with those by ELISA. These results further confirm that the developed UV-vis spectroscopy provides a simple, direct and precise approach for the evaluation of cerebral Aβ monomers.

In conclusion, it is the first time for us to initially develop a direct and simple colorimetric method for the visualization of total amount of soluble Aβ monomers in normal and AD rats,

which makes use of the dual-recognition ability of Cu and hemin functionalized GNPs to specifically bind Aβ monomers. Compared with other established approaches for Aβ monitoring such as ELISA, our strategy retains the powerful features inherent in ELISA (e.g., quantitative, sensitive and selective), but offers other additional advantages, including faster in analysis, obviation of an enzyme-linked antibody for Aβ recognition, theoretically simple, low demands in instrument and visualization. The proof-of-concept experiment demonstrates that UV-vis can potentially serve as a viable alternative for facile and sensitive clinical analysis of important biomarkers related to neurodegenerative diseases such as AD, Huntington's disease and Parkinson's disease.

The author would like to thank NSFC (Grant No. 21205102 and 81402969), Qinglan Project and the Priority Academic Program Development of Jiangsu Higher Education Institutions (PAPD).

Notes and references

[a] *Department of Pharmaceutical Analysis, Xuzhou Medical College, 209 Tongshan Road, Xuzhou 221004, P.R.China.*
[b] *Jiangsu Key Laboratory of New Drug Research and Clinical Pharmacy, Xuzhou Medical College, 209 Tongshan Road, Xuzhou 221004, P.R.China. Email: yinxx@xzmc.edu.cn; Tel: +86 516 8326-2009; Fax: +86 516 8326-2630.*
[c] *Department of Pharmacy, Xuzhou Medical College, 209 Tongshan Road, Xuzhou 221004, P.R.China.*
[d] *Department of Medicinal Chemistry, China Pharmaceutical University, 24 Tongjia Xiang, Nanjing 210009, P.R.China.*
[1] *Yan-yan Yu and Lin Zhang contributed equally to this work.*

† Electronic Supplementary Information (ESI) available: See DOI: 10.1039/b000000x/

1 M. L. Bolognesi, A. Cavalli, L. Valgimigli, M. Bartolini, M. Rosini, V. Andrisano, M. Recanatini and C. Melchiorre, *J Med Chem*. 2007, **50**, 6446-6449.

2 (a) L. M. Billings, S. Oddo, K. N. Green, J. L. McGaugh and F. M. LaFerla, *Neuron*. 2005, **45**, 675-688; (b) D. M. Skovronsky, R. W. Doms and V. M. Lee, *J Cell Biol*. 1998, **141**, 1031-1039; (c) D. M. Walsh and D. J. Selkoe, *Protein Pept Lett*. 2004, **11**, 213-228.

3 (a) W. B. Stine, Jr., K. N. Dahlgren, G. A. Krafft and M. J. LaDu, *J Biol Chem*. 2003, **278**, 11612-11622; (b) C. L. Shen and R. M. Murphy, *Biophys J*. 1995, **69**, 640-651; (c) M. Vestergaard, K. Kerman, M. Saito, N. Nagatani, Y. Takamura and E. Tamiya, *J Am Chem Soc*. 2005, **127**, 11892-11893.

4 (a) C. Wang, D. Liu and Z. Wang, *Chem Commun (Camb)*. 2012, **48**, 8392-8394; (b) C. Wang, D. Liu and Z. Wang, *Chem Commun (Camb)*. 2011, **47**, 9339-9341; (c) N. T. Ditto, T. R. Kline, P. D. Alfinito and J. R. Slemmon, *J. Neurosci. Methods*. 2009, **182**, 260-265; (d) D. G. Georganopoulou, L. Chang, J. M. Nam, C. S. Thaxton, E. J. Mufson, W. L. Klein and C. A. Mirkin, *Proc. Natl. Acad. Sci. U. S. A.*, 2005, **102**, 2273-2276.

5 P. E. Spies, D. Slats, J. M. Sjogren, B. P. Kremer, F. R. Verhey, M. G. Rikkert and M. M. Verbeek, *Curr Alzheimer Res*. 2010, **7**, 470-476.

6 (a) M. Wogulis, S. Wright, D. Cunningham, T. Chilcote, K. Powell and R. E. Rydel, *J Neurosci*. 2005, **25**, 1071-1080; (b) A. J. Veloso, A. M. Chow, H. V. Ganesh, N. Li, D. Dhar, D. C. Wu, S. Mikhaylichenko, I. R. Brown and K. Kerman, *Anal Chem*. 2014, **86**, 4901-4909; (c) M. A. Lovell, J. D. Robertson, W. J. Teesdale, J. L. Campbell and W. R. Markesbery, *J Neurol Sci*. 1998, **158**, 47-52.

7 E. Gaggelli, H. Kozlowski, D. Valensin and G. Valensin, *Chem Rev*. 2006, **106**, 1995-2044.

8 J. W. Karr, L. J. Kaupp and V. A. Szalai, *J Am Chem Soc*. 2004, **126**, 13534-13538.

9 C. C. Curtain, F. Ali, I. Volitakis, R. A. Cherny, R. S. Norton, K. Beyreuther, C. J. Barrow, C. L. Masters, A. I. Bush and K. J. Barnham, *J Biol Chem*. 2001, **276**, 20466-20473.

10 T. Kowalik-Jankowska, M. Ruta, K. Wisniewska and L. Lankiewicz, *J Inorg Biochem*. 2003, **95**, 270-282.

11 D. Pramanik, C. Ghosh and S. G. Dey, *J Am Chem Soc*. 2011, **133**, 15545-15552.

12 B. Kong, A. Zhu, Y. Luo, Y. Tian, Y. Yu and G. Shi, *Angew Chem Int Ed Engl*. 2011, **50**, 1837-1840.

13 S. K. Ghosh and T. Pal, *Chem Rev*. 2007, **107**, 4797-4862.

14 Y. Yu, Y. Yang, H. Gu, T. Zhou and G. Shi, *Biosens Bioelectron*. 2013, **41**, 511-518.

15 J. Shearer and V. A. Szalai, *J Am Chem Soc*. 2008, **130**, 17826-17835.

16 C. S. Atwood, R. C. Scarpa, X. Huang, R. D. Moir, W. D. Jones, D. P. Fairlie, R. E. Tanzi and A. I. Bush, *J Neurochem*. 2000, **75**, 1219-1233.

17 L. Q. Hatcher, L. Hong, W. D. Bush, T. Carducci and J. D. Simon, *J Phys Chem B*. 2008, **112**, 8160-8164.

18 L. Liu, Q. He, F. Zhao, N. Xia, H. J. Liu, S. J. Li, R. L. Liu and H. Zhang, *Biosens Bioelectron*. 2014, **51**, 208-212.

19 (a) R. Picou, J. P. Moses, A. D. Wellman, I. Kheterpal and S. D. Gilman, *Analyst*. 2010, **135**, 1631-1635; (b) N. Xia, L. Liu, M. G. Harrington, J. Wang and F. Zhou, *Anal Chem*. 2010, **82**, 10151-10157.

20 Y. Yu, L. Zhang, C. Li, X. Sun, D. Tang and G. Shi, *Angew Chem Int Ed Engl*. 2014, **53**, 12832-12835.